Original Article

Propagation Properties of a New Human Diploid Cell Line, RAZI-HDC, and Its Suitability as a Candidate Cell Substrate for Respiratory Syncytial Virus Vaccine Production in Comparison to MRC-5

Abbasi, A[1], Mohammadi, A[2], Alirezaie, B[2], Esna-Ashari, F[2], Sadri, N[3], Salimi, V[4*]

1. *Department of Biotechnology, Faculty of Advanced Sciences and Technology, Tehran Medical Sciences, Islamic Azad University, Tehran, Iran.*
2. *Razi Vaccine and Serum Research Institute (RVSRI) Hessark Karadj Agricultural Research, Education and Extension Organization (AREEO), Tehran, Iran.*
3. *Department of Microbiology and Immunology, Faculty of Veterinary Medicine, University of Tehran, Tehran, Iran.*
4. *Department of Virology, School of Public Health, Tehran University of Medical Sciences, Tehran, P.O. Box: 1417613151, Iran.*

How to cite this article: **Abbasi A, Mohammadi A, Alirezaie B, Esna-Ashari F, Sadri N, Salimi V. Propagation Properties of a New Human Diploid Cell Line, RAZI-HDC, and Its Suitability as a Candidate Cell Substrate for Respiratory Syncytial Virus Vaccine Production in Comparison to MRC-5. Archives of Razi Institute. 2025;80(1):51-59.** DOI: 10.32592/ARI.2025.80.1.51

Article Info:
Received: 2 June 2024
Accepted: 31 August 2024
Published: 31 February 2025

Corresponding Author's E-Mail:
vsalimi@tums.ac.ir
vahidsalimii@gmail.com

ABSTRACT

Respiratory syncytial virus (RSV) is a common cause of infection of the respiratory tract in infants, older adults, individuals with heart and lung disease, and immunocompromised patients. The disease is responsible for between 100,000 and 200,000 infant deaths on an annual basis. RSV vaccine production platforms have been developed. In this study, a local diploid cell line, RAZI-HDC, derived from human fetal lung cells, was utilized for RSV virus propagation with the objective of studying live-attenuated vaccine, and was compared to the MRC-5 cell line. The total cells per 25-cm2 flask were 44.0 ± 2.6 *105 and 41.66 ± 2.08 *105 for MRC-5 and RAZI-HDC, respectively. The maximum cell-specific growth rate of RAZI-HDC was 316.66 ± 20.81, while that of MRC-5 was only 340 ± 26.45. The maximum cell division number of RAZI-HDC was 1.24 ± 0.07, in comparison to the MRC-5, with a maximum cell division number of 1.32 ± 0.08. Both cell substrates achieved maximum cell density five days after the initiation of the culture. The complete cytopathic effect of RSV in RAZI-HDC-RAZI-HDC was observed after four days, indicating the sensitivity of these cells to RSV. The virus productivity in RAZI-HDC cells (2.4685) was not significantly different from that in MRC-5 cells (2.5), as determined by a two-tailed t-test (p=0.78). The results indicated that both cell substrates function similarly in terms of RSV propagation. It is noteworthy that diploid cell lines, such as MRC-5 and RAZI-HDC, are particularly well-suited for vaccine manufacturing. This is primarily due to their human origin and the stability of their karyotype. This is a significant advantage, as it helps ensure the safety of the final vaccine product if these cells are used to make viral vaccines that require virus amplification. The study further assessed the replication capacity of the RAZI-HDC cell line and found it to be equivalent to that of the MRC-5 cell line. Specifically, the maximum virus productivity in RAZI-HDC cells (2.4685 log TCID50/mL) was not significantly different from that in MRC-5 cells (2.5 log TCID50/mL), as determined by statistical analysis. The utilization of a locally developed cell line such as RAZI-HDC has the potential to be more cost-effective in comparison to relying on imported cell substrates.

Keywords: RSV, propagation, RAZI-HDC, MRC-5 Cell Line, Vaccine.

1. Introduction

Respiratory Syncytial Virus (RSV) has been identified as the primary cause of acute respiratory infection (ARI) in infants and older adults worldwide, responsible for a significant proportion of hospitalizations and deaths due to lower respiratory tract infections in children under five (1). RSV infection is virtually universal among children by the age of two, with frequent reinfections. In adults, RSV is a significant cause of community-acquired pneumonia, particularly during the winter months, with the potential for progression to respiratory failure or death (2). The substantial infection rate and risk of severe complications underscore RSV as a significant public health challenge and a substantial economic burden. The development of a safe and effective vaccine could play a pivotal role in mitigating severe outcomes, reducing hospitalizations and fatalities, and enhancing the health and well-being of children and at-risk populations. RSV is classified as a member of the pneumovirus genus within the Paramyxoviridae family. It is an enveloped virus with a negative-sense, single-stranded RNA genome ranging from 15,191 to 15,226 nucleotides, which encodes for 11 proteins (3). The virus's main immunogens, the surface glycoproteins F and G, elicit neutralizing antibodies that inhibit viral fusion and binding, respectively. RSV is classified into two antigenic groups, A and B, distinguished by variations in glycoprotein G and other proteins (4). The majority of licensed human viral vaccines, including those for measles, mumps, rubella, rotavirus, varicella, yellow fever, and influenza (nasal), are live attenuated virus forms (5). Live attenuated vaccines (LAVs) have emerged as a promising approach to immunizing children and adults against RSV without inducing the disease. These vaccines are designed to elicit a response akin to a natural infection, thereby inducing active immunization through the stimulation of innate and adaptive immune responses. These vaccines demonstrate limited replication, are well-tolerated, and are the only RSV vaccines demonstrated to be safe in RSV-naïve subjects through studies (6). The development of LAVs involves the selection of viral mutants adapted at low temperatures (cold passage) or through mutagenesis and selection for viruses unable to thrive at higher temperatures (temperature-sensitive mutants) (7). This strategy enables the mutants to replicate in the upper respiratory tract while preventing their growth in the lower respiratory tract, thus averting disease (8). A primary objective in the development of attenuated RSV vaccines is to identify viral mutants that maintain a delicate balance: sufficiently attenuated to avoid causing disease while still robust enough to stimulate the immune system and effectively confer immunity. The advancement of LAVs has been enabled by reverse genetics, a technique that allows for precise modifications and deletions in the RSV genome (9). However, it is imperative to acknowledge the potential influence of the virus's passage on its evolution, as the reverse genetics approach entails the artificial manipulation of genetic material, resulting in mutations that diverge from natural evolutionary processes (10). The selection of an appropriate cell line for the purpose of virus passage is of critical importance in the development of a vaccine for RSV. The selected cell line must facilitate efficient viral replication while ensuring its safety for human application. Historically, vaccines have been developed using various cell substrates, including primary cultures from adult animals, bird tissues, and cell lines. However, the utilization of primary cultures from adult animals is gradually being discontinued due to the occurrence of severe adverse effects. On the other hand, bird tissue substrates have been observed to elicit a lower incidence of local allergic reactions and to result in diminished antibody titers (11). Vero cells, derived from African green monkey kidney cells, have been extensively utilized in the production of inactivated vaccines due to their high viral replication capacity and scalability (12). Nevertheless, concerns persist about potential contamination with non-human DNA, which poses carcinogenic risks and complicates vaccine purification (13,14). Human diploid cells, exemplified by the MRC-5 cell line derived from the lung tissue of a 14-week aborted Caucasian male fetus (15), present a safer alternative. These cells have become increasingly popular for manufacturing viral vaccines, such as those for hepatitis A, varicella, and polio, and they have proven susceptible to RSV (16). However, the MRC-5 cell line exhibits certain limitations, including reduced efficiency and genetic changes due to extensive passage numbers. Consequently, there is an imperative to cultivate an equivalent or superior cell line to ensure the efficacy and reliability of cell-based research and vaccine production. The Razi Vaccine and Serum Research Institute has established a new diploid cell line, designated RAZI-HDC (R-HDC), derived from the lung tissue of a 4-month-old female fetus. The present study aims to make a comparison between the RSV growth rate and proliferation in the R-HDC cell line and that in the MRC-5 cell line. The findings reveal that the growth rates and virus titers of these two cell lines are nearly identical, underscoring the promise of R-HDC as a novel platform for vaccine development and RSV research.

2. Materials and Methods

2.1. Cells

The present study employed three distinct cell lines: Vero, MRC-5, and R-HDC. Vero cells were exclusively employed for viral titration. MRC-5 cells, which are susceptible to a wide range of viruses, are commonly utilized in the production of viral vaccines. The R-HDC cell line was derived from foreskin and dental pulp, which were obtained from the lung tissue of an 18-week-old Iranian female fetus. This cell line was previously developed in our laboratory as part of a study on the development of cell substrates (unpublished data) (17, 18).

2.2. Cell Cultivation

MRC-5 cells were cultivated in Dulbecco's Modified Eagle's Medium (DMEM, Gibco BRL) with an 8% concentration of fetal bovine serum (FBS, Gibco BRL) and

kanamycin-neomycin (Biosera, UK). The cells were seeded at a density of 1×105 cells/ml in cell culture flasks (175 cm2 or 25 cm2) and incubated at 37°C. Subsequent subculturing was performed upon reaching confluence, approximately every four days, involving a wash with phosphate-buffered saline (PBS), followed by detachment using 0.025% trypsin. R-HDC cells were subjected to the same protocol, with Subculturing adjusted to occur every five days.

2.3. Virus

The RSV Long strain, provided by Louis Bont from Wilhelmina Children's Hospital, University Medical Center Utrecht, was utilized in this study. Virus stocks were prepared in Vero cells using DMEM, with 10% FBS added as a supplement. The virus was then used to infect the cells at a low multiplicity of infection (MOI, ~0.001). Viral cultures were harvested upon the observation of maximal cytopathic effect, typically between 3-4 days post-infection. The resulting culture medium was then collected, clarified through a centrifugal process, and stored at a temperature of -80°C.

2.4. Cell Counting by Hemocytometer

Cell density was determined using a hemocytometer. The cells were trypsinized, suspended, and mixed with 0.4% Trypan blue in a clean microtube (50 µl each). The mixture was subsequently enumerated under a microscope using an Improved Neubauer slide (HBG, Germany).

2.5. Cell Growth Kinetics

Growth kinetics were monitored by enumerating the total cells in 25-cm2 flasks at 24-hour intervals. The experiment utilized 24 flasks for either the MRC-5 or R-HDC cell lines, as previously described. The specific cell growth rate, µ (h-1), and cell division number, Cd, were calculated using established methods by Samia Rourou.

2.6. Virus Titers in Terms of log 10TCID 50/mL

Vero cells, following detachment, were seeded in 96-well tissue culture plates using Minimum Essential Medium (MEM) with 10% FBS and 1× antibiotic-antimycotic solution. Following the attainment of confluence, as determined by microscopic observation, the cells were subjected to infection with tenfold serial dilutions of the virus samples in MEM, with the addition of 1.5% BSA to serve as a stabilizing agent. Following a 4-day incubation at 37°C, the presence or absence of cytopathic effects (CPE), including cell rounding, detachment, and lysis, was microscopically evaluated.

2.7. Infection of Cell Monolayer with RSV

The study's authors employed the methods described by Samia Rourou to determine virus growth kinetics. These methods included the modified Koprowski method for virus inoculation. Following the removal of the culture medium, the cell monolayer was washed with phosphate-buffered saline (PBS), and the virus seed was applied in a minimal volume of Dulbecco's modified Eagle medium (DMEM). The monolayer was then subjected to an incubation period of 45 minutes at a temperature of 37°C. This was followed by an additional incubation in a DMEM solution that had been supplemented with 0.2% human albumin.

2.8. Observation of Cytopathic Effect (CPE) in the Infected Cell Cultures

The CPE was monitored daily using an inverted microscope after virus inoculation. The cell culture media from infected cells was then inoculated onto a susceptible VERO cell line to facilitate further validation. After 72 hours at 37°C, the CPE was assessed daily. Post-inoculation, VERO cells were fixed with 30% formalin and stained with crystal violet to enhance visual confirmation.

2.9. Virus Growth Kinetics

In order to analyze virus growth kinetics, six-well plates with either R-HDC or MRC-5 cells at 90% confluence were inoculated in duplicates with a virus seed at a multiplicity of infection (MOI) of 0.01, using 500 µL of medium per well. The cell monolayers were harvested at predetermined times post-infection (6, 24, 48, 72, 96, and 120 hours). The monolayers were scraped into the medium, vortexed, snap frozen in liquid nitrogen, and stored at -80°C until analyzed by the TCID50 assay. The specific virus production rate (P) was determined using the following equation (Eq. 1) (1):

$$P = \frac{Cn + 1 - Cn}{\Delta t}$$

Cn and Cn+1 represent the virus titers in focus-forming units per milliliter (*0.7 FFU/mL) (20) at consecutive time points tn and tn+1, respectively, and Δt is the time interval between these points. The overall virus productivity was calculated using the following equation (Eq. 2) (2):

$$Overall\ Virus\ Productivity = \left(\frac{C}{Xinfection}\right) \times \left(\frac{1}{Xend} - \frac{1}{Xinfection}\right)$$

In this model, CC represents the virus titer in CCID50/mL, obtained at the conclusion of the culture period, Xinfection denotes the cell density at the time of infection, and Xend signifies the cell density at the termination of the culture period, with both densities expressed in cells/mL. The infection time refers to the duration of the virus production phase, expressed in hours.

2.10. Data Analysis

The data were analyzed using GraphPad Prism software and Microsoft Excel. The results obtained from these analyses represent the mean values from three or more independent experiments, with the standard deviations of these values being shown as well. For the purpose of making comparisons between two groups of data that are said to be normally distributed, either the Student's two-tailed t-test or the paired Student's one-tailed t-test was utilized.

3. Results

3.1. Cell Proliferation

The growth dynamics of R-HDC cells were meticulously tracked under static culture conditions within 20Z flasks. Cell counts at successive time points were recorded, and the growth percentage was calculated by comparing the cell count at each time point to the maximum cell count observed during the growth period. The results of this study are summarized in Table 1 and Diagram 1. During the initial eight days of cultivation, the cell counts and percentage growth (mean±SD (*10^5)) in the flasks were as follows: Day 1 - 12±0 (20%), Day 2 - 15.33±0.57 (53.33%), Day 3 - 21.33±2.51 (133.3%), Day 4 - 27±2.64 (170%), Day 5 - 34.6±2.08 (246.66%), Day 6 - 37.33±2.88 (273.33%), Day 7 - 41±1.73 (310%), and Day 8 - 41.66±2.08 (316.66%). The growth rate analysis indicates that the R-HDC strain demonstrated a delayed growth phase from the first to the third day following culture initiation. However, a robust growth phase was observed until the fifth day during the logarithmic phase. Subsequent to the fifth day, the growth rate plateaued, reaching a level comparable to that of the MRC-5 cell line. Consequently, the findings indicate that the optimal time for the passage of R-HDC cells or their utilization in viral inoculation and vaccine preparation is between the fifth and sixth days. A comparison with the standard MRC-5 cell substrate revealed no significant differences, suggesting that R-HDC cells are a suitable alternative for research and production. The number of cell divisions at each time point was also calculated at 24-hour intervals. From the first to the eighth day of culture, the number of cell divisions recorded was 0.32±0.015, 0.51±0.01, 0.69±0.07, 0.83±0.07, 1.02±0.01, 1.17±0.11, 1.21±0.08, and 1.24±0.07, respectively. The majority of cell divisions occur by the seventh day post-passage, indicating uninterrupted cell division until this point. Statistical analysis revealed no significant difference in cell division rates from the fifth to the eighth day ($p<0.05$), suggesting that cell passaging or viral inoculation could be effectively performed during this period. A comparative analysis of cell division rates under static conditions for R-HDC and MRC-5 cells revealed similar behaviors. The specific growth rates were determined by averaging cell counts from three 20Z flasks at 24-hour intervals, as presented in Tables 1. The specific growth rate of R-HDC cells on the eighth day was as follows: 0.0029±0.00920, 0.006±0.0123, 0.0083±0.0108, and 0.0093±0.0098, 0.010 and 0.011±0.0003 μ (h^{-1}). The specific growth rate was initially low and displayed a high standard deviation but gradually increased, reaching its peak during the fifth day. Subsequent to this peak, the growth rate underwent a decline. A comparative analysis of specific growth rates under static conditions revealed that MRC-5 and R-HDC cells function similarly, achieving a dense monolayer by day 5. However, the quality of calf serum can significantly impact this process (Table 1). The R-HDC cell growth curve demonstrated a lag phase on the first day post-culture, followed by logarithmic growth until the day. A comparative analysis of the growth rates of MRC-5 and R-HDC cells over eight days revealed that MRC-5 cells generally exhibited a slightly higher growth rate, though the differences were minimal and not statistically significant (Figure 1). The calculation of cell divisions (Cd) revealed that the majority occurred on the eighth day post-passage, with no significant difference from day six to eight ($p<0.05$) (Figure 2). The specific growth rate (μ) for R-HDC cells was initially the lowest, increasing until it peaked on day seven at an average of 0.012, after which it decreased again. In contrast, the MRC-5 cells demonstrated a rapid specific growth rate from the beginning, reaching a peak on day three at an average of 0.0135. However, a statistically insignificant disparity in growth kinetics was observed between the two cell lines (Figure 3). In summary, R-HDC cells under static culture conditions initially exhibited a delayed growth phase, followed by a logarithmic increase until the fourth day and then a decline. The majority of cell divisions occurred on the eighth day post-passage. The specific growth rate of R-HDC cells gradually peaked on the fourth day. While the growth rate of R-HDC cells was comparable to that of MRC-5, the slight differences observed were not statistically significant.

3.2. Cell Infection Monitoring

The R-HDC and MRC-5 cell lines exhibited evident cytopathic effects (CPE) following inoculation, marked by cellular rounding and detachment. This CPE was observable by the third day post-inoculation and intensified over time (Figure 4.a.b.d.e). Furthermore, the transfer of the infected R-HDC cell's culture medium to VERO cells resulted in a marked CPE, thereby confirming the infectivity and viability of the viruses produced in R-HDC cells. Following inoculation, VERO cells were fixed with 30% formalin and stained with crystal violet, a method that enhances the visibility of the CPE, thereby providing more apparent visual confirmation of the results (Figure 4. c.f). Inoculation with RSV, exhibiting overt indications of CPE, including rounding and detachment. C: VERO cell six days post-inoculation with virus produced in the R-HDC cell line, stained with crystal violet to highlight infected cells. D: Uninfected MRC-5 cells exhibited no signs of cytopathic effect. E: MRC-5 cells six days post-inoculation with RSV, showing clear signs of CPE, including rounding and detachment. The sixth day of inoculation with the virus produced in the MRC-5 cell line resulted in the staining of VERO cells with crystal violet, thereby highlighting infected cells.

3.4. Virus Growth Kinetics

In order to assess the impact of cell substrate on virus productivity, a series of flasks were prepared and inoculated with virus seeds at an MOI of 1/10. These flasks were then incubated using the monolayer method. As was the case in our previous experiment, cell concentrations and virus titers were measured at 24-hour intervals. The specific virus production rate and overall virus productivity were then calculated from these data (Table 2) (17, 18). The virus titers in the MRC-5 and R-HDC cell lines exhibited a consistent increase throughout the incubation period,

Table 1. Growth and Cell Division Metrics of MRC-5 and R-18 Cells over Time

sampling Time (hours after passage)	Total Cell Count Per 25 Cm2 Flask (*10^5) Mean ± SD		% Growth Mean ± SD		Cell Division Number(Cd) Mean ± SD	
	MRC-5	R-18	MRC-5	R-18	MRC-5	R-18
0	10	10	0.0	0.0	0	0
24	12.0 ± 1.0	12±0	26.7±2.2	20±0	0.36±0.03	0.32±0.015
48	15.6 ± 2.1	15.33±0.57	34.8±4.6	53.33±5.77	0.47±0.06	0.51±0.01
72	24.3 ± 2.5	21.33±2.51	54.1±5.6	133.3±25.16	0.73±0.08	0.69±0.07
96	29.6 ± 2.5	27±2.64	196.6±±1.9	170±26.45	0.89±0.08	0.83±0.07
120	36.6 ± 3.7	34.6±2.08	266.6±37.8	246.66±20.81	1.10±0.11	1.02±0.01
144	41.0 ± 4.5	37.33±2.88	310±45.8	273.33±28.86	1.23±0.14	1.17±0.11
168	43.3 ± 2.3	41±1.73	333.3±23	310±17.32	1.30±0.07	1.21±0.08
192	44.0 ± 2.6	41.66±2.08	340±26.45	316.66±20.81	1.32±0.08	1.24±0.07

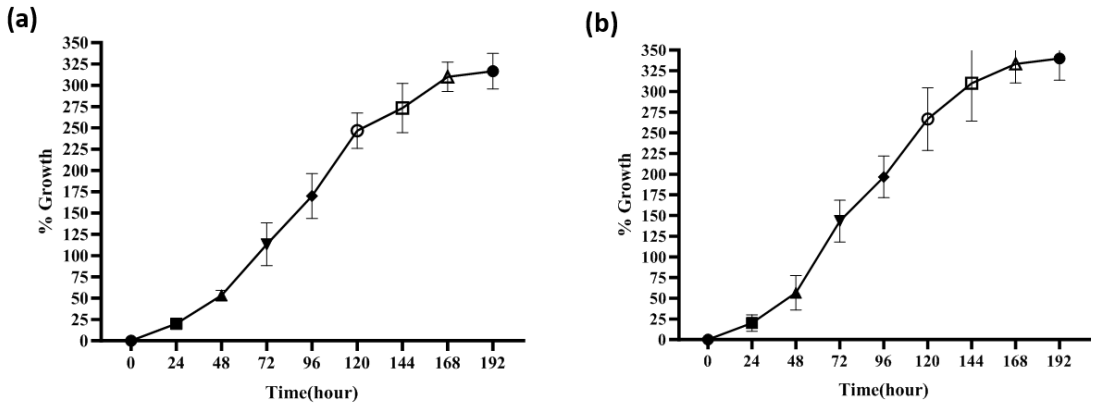

Figure 1: Growth curve of RHDC *(a)* and MRC-5 *(b)* cells under static culture conditions. Cell counts in flasks are plotted against incubation time. Cells were cultured in DMEM with 7% FBS in a 25 cm² flask.

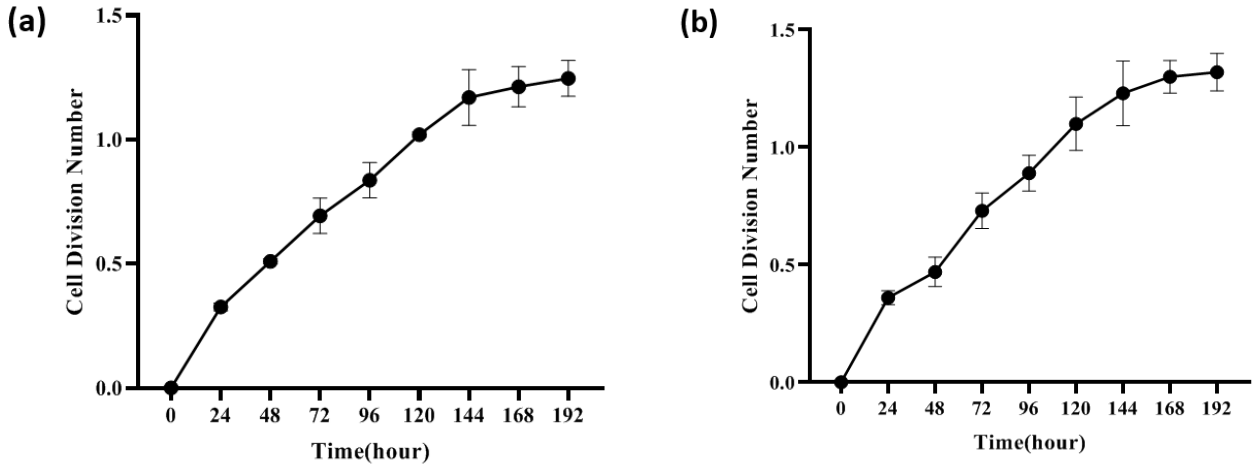

Figure 2: Number of cell divisions over time in static cultures of RHDC *(a)* and MRC-5 *(b)* cells.

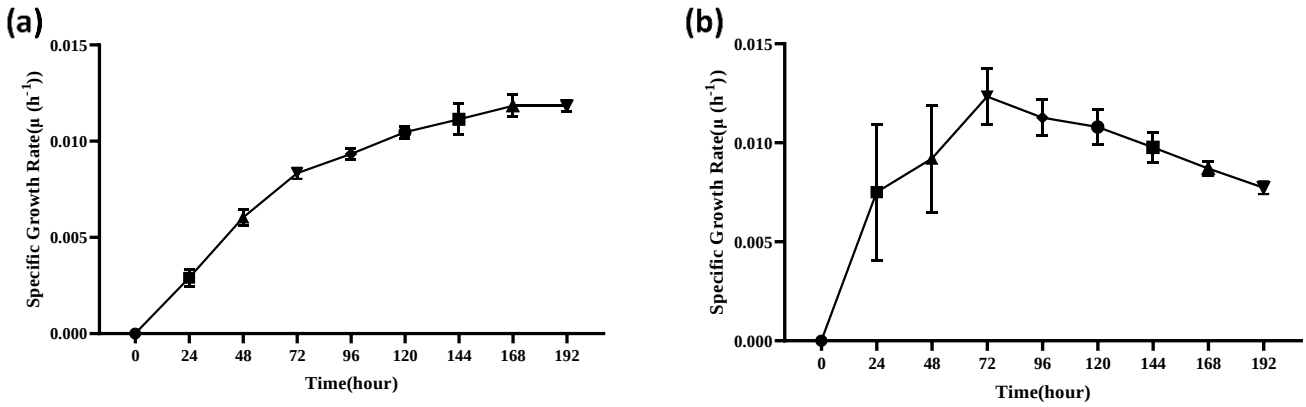

Figure 3: Growth curves for RHDC *(a)* and MRC-5 *(b)* cells at consecutive time points

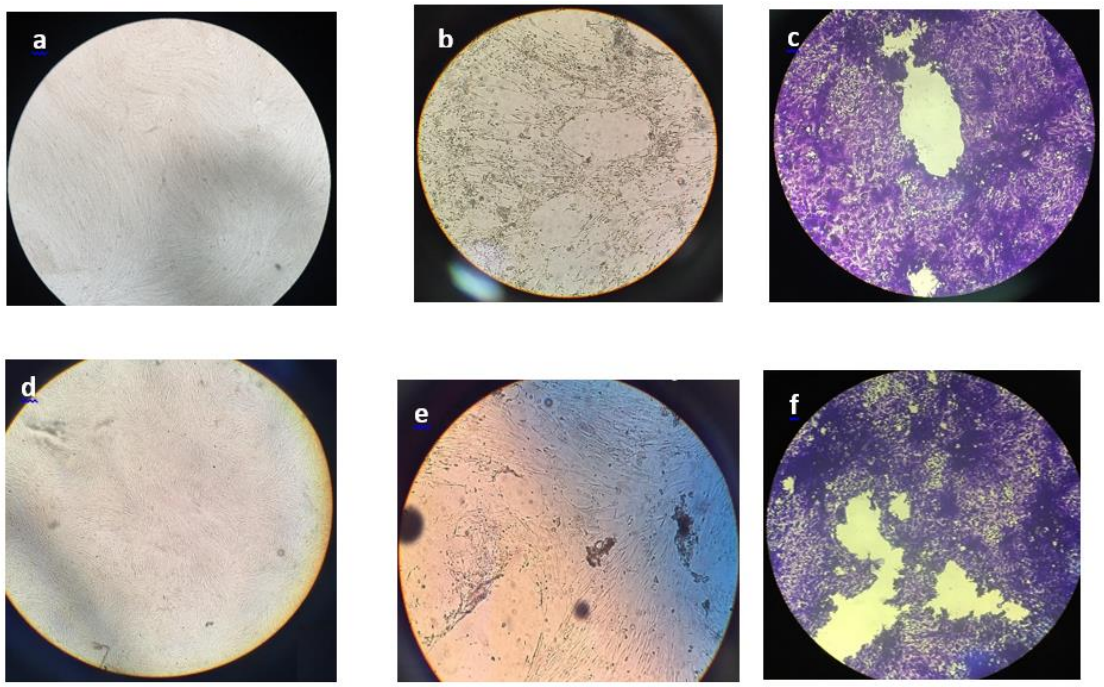

Figure 4: a) An uninfected RHDC cell showing no signs of cytopathic effect. **b)** RHDC 4 days post-infection. **c)** RHDC 4 days post-infection stained with crystal violet. **d)** An uninfected MRC-5 cell showing no signs of cytopathic effect. **e)** MRC-5 4 days post-infection. **f)** MRC-5 4 days post-infection stained with crystal violet

Table 2: Data on virus titer, total cell number, specific virus production rate, and virus productivity at different time points post-virus inoculation for MRC-5 and R-18 cells.

Time After Virus Inoculation	Mean ±SD of Virus Titer in Harvest CCID/50)/ml		Total Cell Count Per/Ml Mean ± SD		Specific Virus Production Rate		Virus Productivity	
Hrs	MRC-5	R-18	410000		CCID50/Cell/H		Mean±SD	
			MRC-5	R-18	MRC-5	R-18	MRC-5	R-18
24	$3.4*10^2$	$3.23*10^2$	$400±100*10^3$	$400±125*10^3$	0.001± 0.0035	0.00092±0.27	0.01394	0.0132
48	$4*10^3$	$3.9*10^3$	$420±40.4*10^3$	$405±41*10^3$	0.08±0.0027	0.11±0.14	0.0032	0.156
72	$4.66*10^4$	$1.527*10^5$	$411±95*10^3$	$400±51.2*10^3$	2.440.0014	1.15±0.14	1.8676	0.2107
96	$5*10^5$	$4.32*10^5$	$390±76.3*10^3$	$396±100*10^3$	3.3±0.0009	1.04±0	2.5	2.4685
120	$5.66*10^5$	$6.07*10^5$	$350± 3.2*10^3$	$396±147.3*10^3$	1.65±0.0008	0.11±0.25	0.159	0.3602
144	$5*10^5$	$5.05*10^5$	$310± 1.1*10^3$	$380±0.1*10^3$	0.52±0.0008	0.13±0.25	0.0345	0.1161

reaching a peak between days 3 and 4. Specifically, the specific virus production rate for MRC-5 cells was initially 0.001±0.0035 CCID50 per cell per hour on day 1, escalating to 3.3±0.0009 CCID50 per cell per hour by day 4. A similar trend was observed in R-HDC cells, which initially exhibited a specific virus production rate of 0.00092±0.27 CCID50 per cell per hour on day 1, increasing to 1.15±0.14 CCID50 per hour by day 3 (Figure 5). Both cell lines demonstrated a substantial decline in cell density over the six-day viral replication period, with cell lysis or rounding and detachment reaching its peak on day 4. The maximum viral productivity was observed at 2.5 for MRC-5 and 2.468571 for R-HDC before a noted decrease in both cell lines, particularly in MRC-5 (Table 2). These values demonstrate the dynamics of virus replication and cell density reduction over time, providing insights into the productivity and efficiency of virus production. The virus growth medium was DMEM,with the addition of 0.2% human albumin. The specific virus production rates for MRC-5 (a) and R-HDC (b) and virus productivity for MRC-5 (c) and R-HDC (d) are depicted. This section delineates the dynamics of viral replication and cytopathic effects in MRC-5 and R-HDC cells.

4. Discussion

This article assesses the capacity of the R-HDC cell line to serve as a novel cell substrate for the production of RSV vaccine candidates. RSV is a predominant pathogen responsible for severe respiratory infections in both young children and older adults, contributing substantially to global morbidity and mortality. The study makes a notable distinction between the growth of RSV in R-HDC cells and the well-established MRC-5 cell line, highlighting the pressing need for a safe and effective vaccine against a virus that places a substantial healthcare burden on the global community. The urgency of developing a reliable RSV vaccine is underscored by the fact that it is a leading cause of respiratory infections in vulnerable demographics, including infants and the elderly (17). In order to better understand the behavior of the RS virus in terms of growth in a new cell substrate and to determine the optimal conditions for virus replication for production or research purposes, it is necessary to determine the growth kinetics of the virus in that cell. To this end, the present study has been designed to investigate the kinetics of the growth and multiplication of RSV on the R-HDC cell substrate. To this end, the study will measure and monitor various factors.

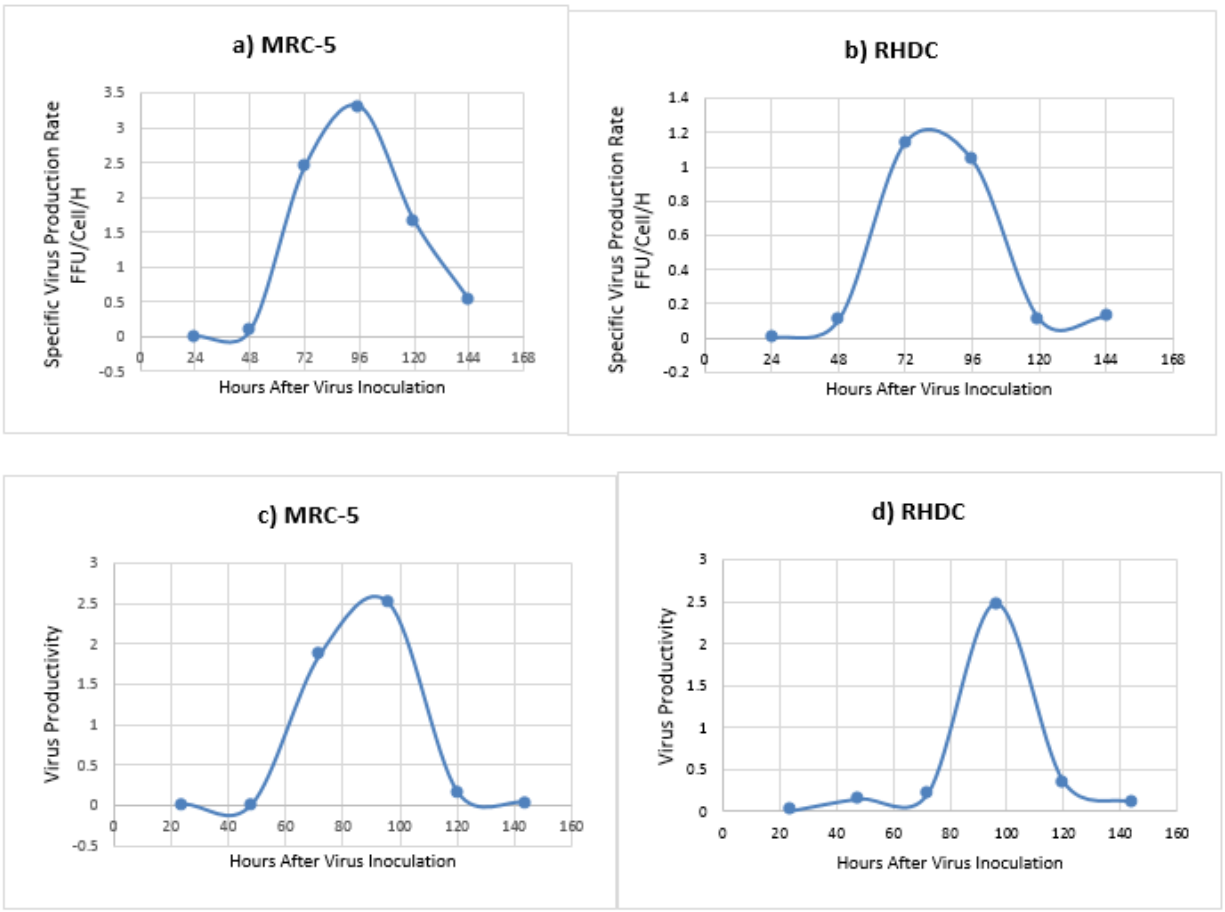

Figure 5: the kinetics of RSV virus production in MRC-5 and R-18 cells under static conditions; Specific virus production rates for MRC-5 (a) and RHDC (b) and virus productivity for MRC-5 (c) and RHDC (d) are depicted.

The most critical of these factors, which include the investigation of the sensitivity of R-HDC cells to RSV, the adaptation of A2 strain RSV virus on R-HDC cells, and the increase of virus titer, were measured in the laboratory. The study's findings, derived from the evaluation of the growth of the respiratory syncytial virus (RSV) on a novel cell substrate, revealed that the virus's growth kinetics are satisfactory when compared to the standard cell line, MRC-5. Maintaining the virus titer and increasing it is imperative for the continuous production of the vaccine, as confirmed through a comparative analysis with the standard cell. The examination of growth kinetics demonstrated R-HDC's viability as a substrate for viral vaccine production, with growth patterns comparable to those of MRC-5 cells. The study further investigates the kinetics of virus growth and productivity of both cell lines following RSV inoculation. The results indicated stable virus titers and comparable specific virus production rates between R-HDC and MRC-5 cells, supporting the efficient replication of RSV within R-HDC cells. These observations offer critical insights into the dynamics of virus replication and cell density reduction over time, parameters that are vital for evaluating the efficiency of vaccine production. The findings indicate that R-HDC cells have the potential to serve as a viable cell substrate for the production of RSV vaccines. The cell line's performance, which was comparable to that of MRC-5 cells in supporting virus growth, underscores its potential as an alternative platform for vaccine development. Future research should optimize culture conditions and evaluate the immunogenicity and efficacy of vaccines produced using the R-HDC cell line in pre-clinical and clinical settings. In conclusion, this study underscores the potential of the R-HDC cell line as a new cell substrate for RSV vaccine production. The study's findings demonstrate the R-HDC cell line's compatibility and efficacy in supporting RSV propagation, paving the way for further exploration of its potential as a safe and reliable substrate for research and development. The results of this study are of significant importance to the ongoing efforts to mitigate the substantial public health impact of RSV through effective vaccine strategies.

Acknowledgment
We extend our profound gratitude to the dedicated professionals of the Human Viral Vaccine department at the Razi Institute, whose insightful contributions have enriched the research process.

Authors' Contribution
Study concept and design: A. M, V. S.
Acquisition of data: A. M, A. A, V. S.
Analysis and interpretation of data: A. M, A. A.
Drafting of the manuscript: A. M, A. A.
Critical revision of the manuscript for important intellectual content: V. S, A. A. A. M.
Statistical analysis: N. S, A. A, A. M.
Administrative, technical, and material support: B. A, F. EA.
Study supervision: V. S, A. M.

Ethics
No animal used in this project

Conflict of Interest
The authors declare that they have no conflict of interest.

Funding
We are appreciative of the financial backing provided by the Razi Vaccine and Serum Research Institutes/Iran for Grant No. 12-18-18-007-000162 from the AREEO.

Author Disclosures
The article submitted to the journal for review is original, authored by the stated authors, and has not been published elsewhere

Data Availability
The necessary data can be obtained from the corresponding author upon reasonable request.

References

1.Shi T, McAllister DA, O'Brien KL, Simoes EA, Madhi SA, Gessner BD, Polack FP, Balsells E, Acacio S, Aguayo C: Global, regional, and national disease burden estimates of acute lower respiratory infections due to respiratory syncytial virus in young children in 2015: a systematic review and modelling study. The Lancet, 2017;390(10098):946-958.
2.Bont L, Checchia PA, Fauroux B, Figueras-Aloy J, Manzoni P, Paes B, Simões EA, Carbonell-Estrany X: Defining the epidemiology and burden of severe respiratory syncytial virus infection among infants and children in western countries. Infectious Diseases And Therapy, 2016;5:271-298.
3.Hayat M, Mohd Yusoff MS, Samad MJ, Abdul Razak IS, Md Yasin IS, Thompson KD, Hasni K: Efficacy of feed-based formalin-killed vaccine of Streptococcus iniae stimulates the gut-associated lymphoid tissues and immune response of red hybrid tilapia. Vaccines, 2021;9(1):51.
4.Nuñez Castrejon AM, O'Rourke SM, Kauvar LM, DuBois RM: Structure-based design and antigenic validation of respiratory syncytial virus G immunogens. Journal of Virology, 2022;96(7):e02201-02221.
5.Seo SH, Jang Y: Cold-adapted live attenuated SARS-Cov-2 vaccine completely protects human ACE2 transgenic mice from SARS-Cov-2 infection. Vaccines, 2020;8(4):584.
6.Karron RA, Atwell JE, McFarland EJ, Cunningham CK, Muresan P, Perlowski C, Libous J, Spector SA, Yogev R, Aziz M: Live-attenuated vaccines prevent respiratory syncytial virus–associated illness in young children. American Journal Of Respiratory And Critical Care Medicine, 2021;203(5):594-603.
7.Jang YH, Seong B-L: Principles underlying rational design of live attenuated influenza vaccines. Clinical And Experimental Vaccine Research, 2012;1(1):35-49.

8.Herfst S, de Graaf M, Schrauwen EJ, Sprong L, Hussain K, van den Hoogen BG, Osterhaus AD, Fouchier RA: Generation of temperature-sensitive human metapneumovirus strains that provide protective immunity in hamsters. Journal Of General Virology, 2008;89(7):1553-1562.
9.Mélade J, Piorkowski G, Touret F, Fourié T, Driouich JS, Cochin M, Bouzidi HS, Coutard B, Nougairede A, de Lamballerie X: A simple reverse genetics method to generate recombinant coronaviruses. EMBO Reports, 2022;23(5):e53820.
10. Durzyńska J, Goździcka-Józefiak A: Viruses and cells intertwined since the dawn of evolution. Virology Journal, 2015;12:1-10.
11. Jordan I, Sandig V: Matrix and backstage: cellular substrates for viral vaccines. Viruses, 2014; 6:1672–1700.
12. Kiesslich S, Kamen AA: Vero cell upstream bioprocess development for the production of viral vectors and vaccines. Biotechnology Advances, 2020;44:107608.
13. Strickler HD, Rosenberg PS, Devesa SS, Hertel J, Fraumeni Jr JF, Goedert JJ: Contamination of poliovirus vaccines with simian virus 40 (1955-1963) and subsequent cancer rates. Jama, 1998;279(4):292-295.
14. Petricciani J, Sheets R: An overview of animal cell substrates for biological products. Biologicals, 2008;36(6):359-362.
15. Zhang K, Na T, Wang L, Gao Q, Yin W, Wang J, Yuan B-Z: Human diploid MRC-5 cells exhibit several critical properties of human umbilical cord-derived mesenchymal stem cells. Vaccine, 2014;32(50):6820-6827.
16. Rodrigues AF, Soares HR, Guerreiro MR, Alves PM, Coroadinha AS: Viral vaccines and their manufacturing cell substrates: New trends and designs in modern vaccinology. Biotechnology Journal, 2015;10(9):1329-1344.
17. Mahmudi - Gharoeie N, Mohammadi A, Saffar B, Esna - Ashari F, Foroghi A, Alirezaee B, Ghorbani R, Sadigh ZA· Development a New Human Skin Continuous Cell Line Sensitive to Mumps Virus: Iranian Journal of Virology 201 3; 7 (4): 7 - 1 3 ©201 3, Iranian Society of Virology
18. Mohammad Taqavian, Mohammad Reza Fazeli, Ahmad Fayaz, Nasrin Samadi, Ashraf Mohammadi, Hooshmand Ilka, Najmeh Mahjoubi: A Novel Cell Substrate Candidate for Rabies Virus Vaccine Propagation and Production. International Journal of eISSN: 2470-9980 Vaccines & Vaccination November 19, 2015
19. Sanjiv R. Shah, Staci R. Kane, Maher Sheikh, and Tensile M. Alfaro: Development of a rapid viability RT-PCR (RV-RT-PCR) method to detect infectious SARS-CoV-2 from swabs. Journal of Virological Methods. 2021 Nov; 297: 114251